Exact Green's function renormalization approach to spectral properties of open quantum systems driven by harmonically time-dependent fields

Liliana Arrachea

Departamento de Física de la Materia Condensada, Universidad de Zaragoza, Pedro Cerbuna 12, (50009) Zaragoza, Spain and Instituto de Biocomputación y Física de Sistemas Complejos, Universidad de Zaragoza, Corona de Aragón 42, (50009) Zaragoza, Spain

(Received 10 May 2006; revised manuscript received 4 August 2006; published 11 January 2007)

We present an efficient method and a fast algorithm to exactly calculate spectral functions and one-body observables of open quantum systems described by lattice Hamiltonians with harmonically time-dependent terms and without many-body interactions. The theoretical treatment is based in Keldysh nonequilibrium Green's function formalism. We illustrate the implementation of the technique in a paradigmatic model of a quantum pump driven by local fields oscillating in time with one and two harmonic components.

DOI: 10.1103/PhysRevB.75.035319 PACS number(s): 72.10.−d, 73.23.−b, 73.63.−b

I. INTRODUCTION

The study of quantum systems in the presence of time-dependent periodic fields is gaining increasing interest within the communities of condensed matter and molecular physics. Of particular experimental relevance are mesoscopic and nanosize devices where electronic and spin transport is originated or influenced by the action of ac fields. Examples are quantum pumps generated by means of ac potential gates oscillating with a phase lag,[1] Aharanov-Bohm rings made of metallic and semiconducting structures, which are threaded by magnetic fluxes with static and harmonically time-dependent components,[2] as well as surface acoustic waves in carbon nanotubes.[3] Other interesting phenomena originated in time-dependent periodic fields are the photovoltaic effect in semiconducting and polymeric heterostructures[4] and the dynamical Franz-Keldysh effect in semiconductors.[5]

An important characteristic of most of these systems is that they are open quantum systems, i.e., they are finite many-particle systems that do not operate isolated but in contact with particle reservoirs. Keldysh nonequilibrium Green's function formalism is a suitable approach to deal with these kinds of setups. The main characteristic of this technique is that it considers the time evolution of a quantum state along a two-way path that begins in $-\infty$, draws forward to $+\infty$, and then backward to $-\infty$. The Green's function is represented by a two-by-two matrix in terms of which perturbation theory has the same structure as in equilibrium many-particle systems. In particular, the evolution of the Green's function is governed by a matricial Dyson equation. A useful representation of this Green's function is defined in terms of retarded and lesser components, which read, respectively,

$$G^R_{l,m}(t,t') = -i\Theta(t-t')\langle\{c_l(t),c^\dagger_m(t')\}\rangle,$$

$$G^<_{l,m}(t,t') = i\langle c^\dagger_m(t')c_l(t)\rangle. \quad (1)$$

In stationary problems, the two Green's functions defined in Eq. (1) depend on the difference between the two times $t-t'$. Hence, the most convenient procedure to evaluate them is to perform a Fourier transform to the frequency space, which, in practice, reduces the set of coupled integral or integro differential Dyson equations to a set of linear equations. This enormous simplification of the problem is a consequence of the fact that the dynamics of the system does not depend on the observational time t (or t') at which the relevant many-body scattering events finish or begin, but rather on what happens in between. This picture is no longer true in the case of systems that depend explicitly on time, where the observational time is also relevant. In such cases, the Green's functions depend on the two times (t,t') or, alternatively, on $(t,t-t')$, or $(t-t',t')$. Within this context, harmonically time-dependent problems constitute very particular cases: although they are not stationary, the time-dependent pattern periodically repeats.

In recent papers, we have presented an approach based in nonequilibrium Green's function formalism to describe the transport properties of systems driven by harmonically time-dependent fields.[6–8] This approach is essentially the formulation of usual Keldysh formalism for particular problems described by Hamiltonians of noninteracting fermions with time-periodic terms. The strategy consists on a convenient choice of the integral representation of Dyson equation for the retarded Green's function, as well as the introduction of the Fourier transform in the difference of time $t-t'$. The latter step takes care of causality and constitutes a natural generalization to the usual procedure carried out for equilibrium and stationary problems. The goal of the treatment is to obtain a set of linear equations in frequency space, analogous to the corresponding ones for equilibrium and stationary problems. There are, however, two main distinctive features: (i) Unlike their equilibrium counterparts, these equations are not diagonal in frequency but rather coupled in quanta of the elementary frequency $\Omega_0=2\pi/\tau_0$, being τ_0 the period defining the time oscillations of the Hamiltonian. (ii) This set of equations depends periodically on the observational time t (or t'), indicating that the ensuing solutions can be represented in terms of Fourier series. Because of the coupling between frequencies, this set contains a large number of equations and can be computationally hard in the case of Hamiltonians with several time-dependent terms and several harmonic components. The aim of this work is to present a fast and computationally low-demanding method to solve such a set of equations. The philosophy is similar to the one used in recursive methods to formulate solutions of the Dyson equation in real space for stationary regimes.[18–23]

 ©2007 The American Physical Society

namely, the elimination of coordinates and equations with the subsequent renormalization of some coupling constants and Green's functions. In the present case, such elimination is defined in frequency coordinates instead of lattice coordinates. The work is organized as follows: In Sec. II, we present the properties of the underlying model and formulate Dyson equations for the Green's functions. In Sec. III, we discuss some important spectral properties of these functions. The algorithm to solve the set of equations for the retarded Green's functions is presented in Sec. IV. In Sec. V, we illustrate the method in a paradigmatic model of quantum pump with biharmonic modulation. Finally, Sec. VI is devoted to summary and conclusions.

II. GENERAL FORMALISM

In this section, we review and generalize the procedure that we have followed to study the transport behavior of a ring threaded by a magnetic field with a linear dependence on time[6] and a model for local pumping potentials.[7,8] The first one can be described in terms of a tight-binding Hamiltonian with a harmonically time-dependent hopping matrix element along one of the bonds, whereas the latter contains local harmonically time-dependent potentials. The generalization presented in what follows considers, in addition, the possibility of ac voltages applied at the reservoirs.

We consider a many-particle system of noninteracting fermions in a finite lattice of N sites, described by a Hamiltonian of the general form

$$H^{\mathrm{sys}}(t) = \sum_{l,l'=1}^{N} (H^{\mathrm{sys}}_{l,l'}(t) c^{\dagger}_{l} c_{l'} + \mathrm{H.c.}), \tag{2}$$

with matrix elements containing stationary and time-periodic components $H^{\mathrm{sys}}_{l,l'}(t) = \varepsilon_{l,l'} + V_{l,l'}(t)$, being $V_{l,l'}(t) = \sum_{k\neq 0} e^{-ik\Omega_0 t} V_{l,l'}(k)$. Let us consider that such a system is connected to M reservoirs through contact terms of the form

$$H^{\mathrm{cont}} = -\sum_{\alpha=1}^{M} w_{\alpha} (c^{\dagger}_{r_\alpha} c_{j_\alpha} + \mathrm{H.c.}), \tag{3}$$

where r_α and j_α are, respectively, coordinates of the reservoirs and the central system.

We generalize the models for reservoirs considered in previous works[6–8] and assume that the corresponding Hamiltonians can also have a harmonical time dependence. On physical grounds, this situation corresponds to external leads under the action of ac voltages,

$$H^{\mathrm{res}}(t) = \sum_{\alpha=1}^{M} \varepsilon_{r_\alpha}(t) c^{\dagger}_{r_\alpha} c_{r_\alpha}, \tag{4}$$

with $\varepsilon_{r_\alpha}(t) = \varepsilon^0_\alpha + V_\alpha \cos(\Omega_0 t)$. An alternative formulation of this problem is attained by performing the gauge transformation: $c_{r_\alpha} \to \bar{c}_{r_\alpha}(t) = c_{r_\alpha} e^{-i\int_{t_0}^{t} dt_1 V_\alpha \cos(\Omega_0 t_1)}$, which transforms $\varepsilon_{r_\alpha}(t) \to \bar{\varepsilon}_{r_\alpha} = \varepsilon^0_{r_\alpha}$ in H^{res} and $w_\alpha \to \overline{w_\alpha}(t) = e^{i\int_{t_0}^{t} dt_1 V_\alpha \cos(\Omega_0 t_1)}$ in H^{cont}. In any case, following the standard procedure introduced in Refs. 15–17, the degrees of freedom of the reservoirs may be integrated out defining the self-energies

$$\Sigma^{<,>}_{l,l'}(t,t') = \pm i \sum_{\alpha=1}^{M} \delta_{l,j_\alpha} \delta_{l',j_\alpha} \sum_{k=-\infty}^{\infty} e^{-ik\Omega_0 t} \times \int_{-\infty}^{\infty} \frac{d\omega}{2\pi} \Gamma^{<,>}_{\alpha}(k,\omega) e^{-i\omega(t-t')}$$

$$\Sigma^{R}_{l,l'}(t,t') = \sum_{\alpha=1}^{M} \delta_{l,j_\alpha} \delta_{l',j_\alpha} [\Sigma^0_{j_\alpha}(t-t') + \bar{\Sigma}_{j_\alpha}(t,t')]$$

$$= \sum_{\alpha=1}^{M} \delta_{l,j_\alpha} \delta_{l',j_\alpha} \int_{-\infty}^{\infty} \frac{d\omega}{2\pi} e^{-i\omega(t-t')} [\Sigma_{j_\alpha}(0,\omega) + \sum_{k\neq 0} e^{-ik\Omega_0 t} \Sigma_{j_\alpha}(k,\omega)], \tag{5}$$

where

$$\Sigma_{j_\alpha}(k,\omega) = \int_{-\infty}^{\infty} \frac{d\omega'}{2\pi} \frac{\Gamma_\alpha(k,\omega')}{\omega - \omega' + i0^+}, \tag{6}$$

with $\Gamma_\alpha(k,\omega) = \Gamma^{<}_{\alpha}(k,\omega) + \Gamma^{>}_{\alpha}(k,\omega)$, being

$$\Gamma^{<,>}_{\alpha}(k,\omega) = |w_\alpha|^2 \sum_{s} J_s\left(\frac{V_\alpha}{\Omega_0}\right) J_{s+k}\left(\frac{V_\alpha}{\Omega_0}\right) \times \rho_\alpha(\omega - s\Omega_0) \lambda^{<,>}_{\alpha}(\omega - s\Omega_0), \tag{7}$$

with $\lambda^{<}_{\alpha}(\omega) = f_\alpha(\omega)$, and $\lambda^{>}_{\alpha}(\omega) = 1 - f_\alpha(\omega)$. The Fermi function $f_\alpha(\omega) = 1/(e^{\beta_\alpha(\omega-\mu_\alpha)}+1)$ depends on the temperature $1/\beta_\alpha$ and chemical potential μ_α of the reservoir α, while $\rho_\alpha(\omega)$ is its equilibrium density of states, i.e., corresponding to $H_{\mathrm{res}}(V_\alpha = 0)$. The function $J_m(x)$ is the Bessel function of order m.

According to Refs. 6–8, we work with the following integral representation of the Dyson equation for the lesser and retarded Green's functions:

$$G^{<}_{l,l'}(t,t') = \sum_{\alpha=1}^{M} \int dt_1 dt_2 G^{R}_{l,j_\alpha}(t,t_1) \Sigma^{<}_{j_\alpha}(t_1 t_2) G^{A}_{j_{\alpha'},l'}(t_2,t') \tag{8}$$

$$G^{R}_{l,l'}(t,t') = G^{0}_{l,l'}(t-t') + \sum_{\alpha=1}^{M} \int dt_1 dt_2 G^{R}_{l,j_\alpha}(t,t_1) \bar{\Sigma}_{j_\alpha}(t_1 t_2) G^{0}_{j_{\alpha'},l'}(t_2 - t') + \sum_{l_1,l_2} \int dt_1 G^{R}_{l,l_1}(t,t_1) V_{l_1 l_2}(t_1) G^{0}_{l_2,l'}(t_1 - t'), \tag{9}$$

where $G^{A}_{l,l'}(t,t') = [G^{R}_{l',l}(t',t)]^*$, and define the following Fourier transform:

$$G^{R}_{l,l'}(t,t') = \int_{-\infty}^{\infty} \frac{d\omega}{2\pi} e^{-i\omega(t-t')} G^{R}_{l,l'}(t,\omega),$$

$$G^R_{l,l'}(t,\omega) = \int_{-\infty}^{t} dt' e^{i(\omega+i0^+)(t-t')} G^R_{l,l'}(t,t'). \tag{10}$$

Note that Eq. (10), in practice considers that $(t,t-t')$ are the natural coordinates to describe the time evolution. For stationary problems, (10) reduces to the usual Fourier transform defined in equilibrium Green's function formalism, which implies that the transformed functions have well-defined analytical properties in the frequency space.[24] Another approach based in Keldysh formalism used in the problem of a single pumping potential oscillating with a single frequency[25] considered a double Fourier transform in t and t', which results in being formally more cumbersome. Other theoretical treatments that, as in our case, consider the observational time and the difference of times as the natural temporal coordinates to describe the dynamics rely on Floquet representation for the Hamiltonian and the wave functions.[12–14]

From Eq. (8), it is clear that the evaluation of the retarded Green's function also provides the solution for the lesser function. Performing the Fourier transform in (9) results in the following set:

$$\hat{G}^R(t,\omega) = \hat{G}^0(\omega) + \sum_{k\geq 1} [e^{-ik\Omega_0 t}\hat{G}^R(t,\omega+k\Omega_0)\hat{V}^-_k(\omega)\hat{G}^0(\omega) + e^{ik\Omega_0 t}\hat{G}^R(t,\omega-k\Omega_0)\hat{V}^+_k(\omega)\hat{G}^0(\omega)], \tag{11}$$

where $\hat{G}^R(t,\omega)$ $[\hat{G}^0(\omega)]$ denotes the $N\times N$ matrix with elements $G^R_{l,l'}(t,\omega)$ $[G^0_{l,l'}(\omega)]$. Analogously, $\hat{V}^{\pm}_k(\omega)=\hat{V}(\mp k)+\hat{\Sigma}(\mp k,\omega)$, where $\hat{V}(k)$ and $\hat{\Sigma}(k,\omega)$ are matrices with elements $V_{l,l'}(k)$ and $\delta_{l,j_\alpha}\delta_{l',j_\alpha}\Sigma_{j_\alpha}(k,\omega)$. The equilibrium Green's function $\hat{G}^0(\omega)$ is the solution of the following Dyson equation:

$$\hat{G}^0(\omega)[\omega\hat{1}-\hat{\varepsilon}-\hat{\Sigma}^0(\omega)] = \hat{1}, \tag{12}$$

where the matrices $\hat{\Sigma}^0(\omega)$ and $\hat{\varepsilon}$ have elements $\Sigma^0_{l,l'}(\omega)=\delta_{l,j_\alpha}\delta_{l',j_\alpha}\Sigma_{j_\alpha}(0,\omega)$, and $\varepsilon_{l,l'}$, respectively.

Because of the time-periodic structure of the set (11), the retarded Green's function is also a periodic function of time and can be expanded in Fourier series

$$\hat{G}^R(t,\omega) = \sum_{k=-\infty}^{\infty} \hat{\mathcal{G}}(k,\omega)e^{-ik\Omega_0 t},$$

$$\hat{\mathcal{G}}(k,\omega) = \frac{1}{\tau_0}\int_0^{\tau_0} dt e^{ik\Omega_0 t}\hat{G}^R(t,\omega). \tag{13}$$

Transforming (11) according to (13) results in

$$\hat{\mathcal{G}}(k,\omega) = \hat{G}^0(\omega)\delta_{k,0} + \sum_{k_1\geq 1} [\hat{\mathcal{G}}(k-k_1,\omega+k_1\Omega_0)\hat{V}^-_{k_1}(\omega)\hat{G}^0(\omega) + \hat{\mathcal{G}}(k+k_1,\omega-k_1\Omega_0)\hat{V}^+_{k_1}(\omega)\hat{G}^0(\omega)]. \tag{14}$$

The structure of Eqs. (11) and (14), in particular, the coupling of different energies that differ in integer numbers of the energy quantum Ω_0, resembles the problem of electrons coupled to quantized phonon or photon fields. This feature has been identified as the source of heating in the problem of a dissipative metallic ring threaded by a time-dependent flux[6,9] and has also been stressed in the context of formulations based in the Floquet representation.[10–13]

In previous works,[6–8] we have considered a frequency cutoff $\pm K\Omega_0$, with large K in (11), such that $K\Omega_0 \gg W$, being W the bandwidth of the system associated to $\hat{G}^0(\omega)$ (i.e., $\mathrm{Im}[\hat{G}^0(\omega)]\sim 0$, for $|\omega|>W$). The corresponding linear set can be numerically solved at different times within the interval $0\leq t\leq \tau_0$. For small amplitudes $V_{l,l'}(k)$ and $\Gamma(k,\omega)$, it is also possible to perform systematic perturbative approximations to the solutions.[7,8] However, the complete evaluation of $G^R(t,\omega)$ for arbitrary amplitudes may involve the manipulation of a formidable large and dense linear set in cases where $V_{l,l'}(t)\neq 0$ for several lattice positions (l,l') and contains more than one harmonic component. On another hand, the computation of the Fourier components $\hat{\mathcal{G}}(k,\omega)$ must be performed numerically *a posteriori*. An alternative procedure would be the evaluation of (14). This would imply solving the set of equations only once and would allow for the direct evaluation of the Fourier components. However, the size of the corresponding matrix is even much larger than in the previous case. The recursive method that we present in Sec. IV circumvent these shortcomings. Although it is based in a systematic elimination of frequency modes in Eq. (11), it allows for the direct evaluation of the Fourier components $\hat{\mathcal{G}}(k,\omega)$ on the basis of operations with matrices of size $N\times N$.

III. SPECTRAL PROPERTIES AND EXPECTATION VALUES OF ONE-BODY OBSERVABLES

Before presenting the method to solve the set (11), we present a discussion on some salient properties of the functions $\hat{\mathcal{G}}(k,\omega)$. As in the case of equilibrium Green's functions, the analytical properties of these functions follow from general principles.

One of the most important properties of equilibrium Green's is the spectral representation,

$$\hat{G}^R(\omega) = \int_{-\infty}^{\infty} \frac{d\omega'}{2\pi}\frac{\hat{\rho}(\omega')}{\omega-\omega'+i0^+}, \tag{15}$$

being $\hat{\rho}(\omega)=\hat{G}^R(\omega)-[\hat{G}^R(\omega)]^\dagger$, the spectral density matrix. From the very definition, the retarded Green's function is related to the lesser Green's function through

$$\hat{G}^R(t,t') = \Theta(t-t')[\hat{G}^>(t,t')-\hat{G}^<(t,t')], \tag{16}$$

being $\hat{G}^>(t,t')=[\hat{G}^<(t',t)]^\dagger$, where $\hat{G}^{>,<}(t,t')$ and $\hat{G}^R(t,t')$ are matrices with elements $G^{>,<}_{l,l'}(t,t')$ and $G^R_{l,l'}(t,t')$, respectively. In equilibrium, these Green's functions are further related in frequency through

$$\hat{G}^<(\omega) = if(\omega)\hat{\rho}(\omega),$$

$$\hat{G}^{>}(\omega) = -i[1 - f(\omega)]\hat{\rho}(\omega). \tag{17}$$

In Eq. (17), we do not indicate any label of reservoir in $f(\omega)$ because at equilibrium all the reservoirs have the same chemical potential and temperature. In addition, due to the anticommutation rules of fermionic operators, $G^R_{l,l'}(t^+,t) = \delta_{l,l'}$, implying the important sum rule

$$\int_{-\infty}^{\infty} \frac{d\omega}{2\pi} \rho_{l,l'}(\omega) = \delta_{l,l'}, \tag{18}$$

which motivates the interpretation of the function $\rho_{l,l}(\omega)$ as a probability distribution function or a local density of states.

On another hand, the identities (17) introduce relations between the matrix elements of the spectral density and the expectation values of one-body observables,

$$\langle c^\dagger_l(t) c_{l'}(t)\rangle = -iG^<_{l',l}(t,t) = \int_{-\infty}^{\infty} \frac{d\omega}{2\pi} f(\omega)\rho_{l',l}(\omega). \tag{19}$$

Note that in equilibrium, the above expectation values do not actually depend on time.

We now turn to discuss the spectral properties of the nonequilibrium retarded Green's function. Performing the Fourier transform and the expansion (13) in the Dyson equation for the lesser (bigger) Green's function (8) and substituting the resulting expression in (16), it is verified

$$\hat{\mathcal{G}}(k,\omega) = \sum_{k_1 k_2 = -\infty}^{\infty} \int_{-\infty}^{\infty} \frac{d\omega'}{2\pi} \frac{\hat{\mathcal{G}}(k - k_2 + k_1, \omega' + k_2\Omega_0)\hat{\Gamma}(k_2,\omega')\hat{\mathcal{G}}^\dagger(k_1,\omega')}{\omega - (\omega' + k_1\Omega_0) + i0^+}. \tag{20}$$

On the other hand, the expectation values of one-body operators are related to the lesser function through: $\langle c^\dagger_l(t)c_{l'}(t)\rangle = -iG^<_{l',l}(t,t)$ and, being periodic functions of time, they can be expressed as

$$\langle c^\dagger_l(t)c_{l'}(t)\rangle = \sum_k e^{-ik\Omega_0 t}\mathcal{N}_{l,l'}(k). \tag{21}$$

Taking into account the Dyson equation (8) and the Fourier representation (13) for the retarded function, the above-defined Fourier component can be expressed as follows:

$$\mathcal{N}_{l,l'}(k) = \sum_{\alpha=1}^{M} \sum_{k_1,k_2=-\infty}^{\infty} \frac{d\omega}{2\pi} \mathcal{G}_{l',j_\alpha}(k - k_2 + k_1, \omega + k_2\Omega_0) \times \Gamma^<_\alpha(k_2,\omega)\mathcal{G}_{l,j_\alpha}(k_1,\omega)^*. \tag{22}$$

The representation of the Green's function (20) evaluated at $k=0$ and its comparison to the corresponding representation at equilibrium given in Eq. (15) allows us to define the dc component of the spectral density matrix:

$$\hat{\rho}(0,\omega) = \sum_{k=-\infty}^{\infty} \hat{\mathcal{A}}(k, \omega - k\Omega_0), \tag{23}$$

$$\hat{\mathcal{A}}(k,\omega) = \sum_{k'=-\infty}^{\infty} \hat{\mathcal{G}}(k - k', \omega + k'\Omega_0)\hat{\Gamma}(k',\omega)\hat{\mathcal{G}}^\dagger(k,\omega). \tag{24}$$

As in equilibrium, fermionic anticommutation rules determine the sum rule,

$$\int_{-\infty}^{\infty} \frac{d\omega}{2\pi} \rho_{l,l'}(0,\omega) = \sum_{k=-\infty}^{\infty} \int_{-\infty}^{\infty} \frac{d\omega}{2\pi} \mathcal{A}_{l,l'}(k,\omega) = \delta_{l,l'}. \tag{25}$$

However, relations such as (17) and (19) are, in general, not expected to be recovered.

An open system driven out of equilibrium through the application of time-dependent local fields, but in contact with stationary reservoirs with the same temperatures and chemical potentials, realizes the situation that is closest to equilibrium within the family that we are considering in the present work. In what follows, we focus on this particular but important case. It can be seen that the expectation value of one-body operators averaged over one period $\overline{\langle c^\dagger_l c_{l'}\rangle} \equiv \mathcal{N}_{l,l'}(0)$ can be expressed in terms of a spectral "density of occupation" matrix $\hat{\bar{\rho}}(0,\omega)$ as

$$\overline{\langle c^\dagger_l c_{l'}\rangle} = \int_{-\infty}^{\infty} \frac{d\omega}{2\pi} f(\omega)\bar{\rho}_{l',l}(0,\omega)$$

$$\hat{\bar{\rho}}(0,\omega) = \sum_{k=-\infty}^{\infty} \hat{\mathcal{A}}(k,\omega), \tag{26}$$

where the matrix $\hat{\mathcal{A}}(k,\omega)$ reduces in this particular case to

$$\hat{\mathcal{A}}(k,\omega) = \hat{\mathcal{G}}(k,\omega)\hat{\Gamma}^0(\omega)\hat{\mathcal{G}}^\dagger(k,\omega), \tag{27}$$

being $\Gamma^0_{l,l'}(\omega) = \Sigma^M_{\alpha=1}\delta_{l,j_\alpha}\delta_{l',j_\alpha}|w_\alpha|^2\rho_\alpha(\omega)$. From Eqs. (26) and (27), we see that, unlike the equilibrium case, $\bar{\rho}_{l,l'}(0,\omega) \neq \rho_{l,l'}(0,\omega)$. By comparing (23) to (26), it becomes, however, apparent that these two spectral densities differ only in energy shifts in the arguments of the coefficients of their Fourier representation. Hence, it is easy to see that the function $\bar{\rho}_{l,l'}(0,\omega)$ satisfies the same sum rule (25).

We shall analyze the above spectral representations in connection to two important observables in systems in contact to stationary reservoirs at the same temperatures and chemical potentials. The first one is the local mean occupation number $n_l=\overline{\langle c_l^\dagger c_l\rangle}$, which is related to the diagonal element of the spectral density of occupation matrix $\bar{\rho}_{l,l}(0,\omega)$. Note that, in the case of stationary reservoirs, $\mathcal{A}_{l,l}(k,\omega)$ is a positive defined function and can thus be interpreted as the local density of states associated to the Fourier component, or "sideband," labeled by k. Hence, the spectral density $\bar{\rho}_{l,l}(0,\omega)$ defined in (26) corresponds to the superposition of all the local densities of states of the different sidebands. Similarly, the spectral density $\rho_{l,l}(0,\omega)$, as defined in (23), corresponds to the superposition of all the local densities of states of the different sidebands with the energies shifted in an amount equal to the associated quanta $k\Omega_0$.

Attempts can be found in the literature of generalizations of the concept of the spectral density of states to out-of-equilibrium situations. In the context of optical properties of semiconductors and Franz-Keldysh effect,[26] as well as in mesoscopic time-dependent transport,[16] a time-dependent "generalized density of states" equal to $-2\,\mathrm{Im}\,G^R_{l,l}(t,\omega)$ has been defined. The corresponding dc component would coincide with $\rho_{l,l}(0,\omega)$, defined in Eq. (23). The different spectral representations analyzed in this section suggest that the Fourier component $\mathcal{A}_{l,l}(k,\omega)$ is a useful function to describe the one-particle dc spectral properties. In fact, as a function of k, this function provides a picture of the relative spectral weight of the different k components, while as a function of ω, it provides a picture of the available states within a given sideband. As stressed before, it is a positive defined function that integrates in k and ω to one. On another hand, if we are interested in working with functions having an actual direct relation to the electronic population, as in, e.g., photoemission spectroscopy or any other experiment devoted to obtaining the energy-resolved electronic population, (e.g., Ref. 27), the occupation spectral density $\bar{\rho}_{l,l}(0,\omega)$ (26), which is directly related to the dc-local occupation number is the natural spectral function to work with. Let us also mention that definitions related to the spectral density of occupation given in Eq. (26) can also be found in the literature. In particular, note that the function $\bar{\rho}_{l,l}(0,\omega)$ is the dc generalization of the function named total energy distribution (TED), defined in Ref. 28 in the context of interacting one-dimensional systems driven by a static bias, and it is close to the the Wigner representation of the TED function given in Ref. 29 in the context of one-dimensional systems with a time-dependent local potential.

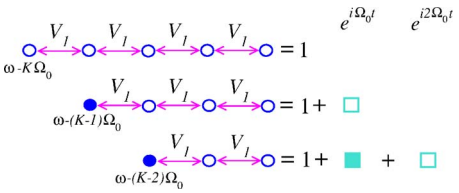

FIG. 1. (Color online) Scheme of the first steps of the low-frequency mode elimination for a time-periodic Hamiltonian with a single harmonic component. Each circle represents the left-hand side of a set of equations centered at a given frequency mode. The squares at the right-hand side represent terms proportional to $e^{im\Omega_0 t}$, with $m=0,1,2$ (from left to right). The renormalized terms are indicated in filled symbols.

The second important observable that we want to analyze in terms of the spectral representation (26) is the induced dc current flowing through the bond $(l,l+1)$ of the driven structure, which is defined as

$$J_l^{dc}=2\,\mathrm{Im}\,\overline{[H^{\mathrm{sys}}_{l,l+1}(t)\langle c_l^\dagger c_{l+1}\rangle]}. \tag{28}$$

For reservoirs with identical chemical potentials and temperatures and the Hamiltonian $H^{\mathrm{sys}}(t)$ defined in (2) with N_p local potentials $V_{l,l'}(t)=\delta_{l,l'}\Sigma_{j=1}^{N_p}\delta_{l,l_j}V_j(t)$ and $\varepsilon_{l,l'}=E_l\delta_{l,l'}-w\delta_{l+1,l'}$, the above current reads

$$J_l^{dc}=-2w\,\mathrm{Im}\left[\int_{-\infty}^{\infty}\frac{d\omega}{2\pi}f(\omega)\bar{\rho}_{l+1,l}(0,\omega)\right]$$
$$=-2w\sum_{k=-\infty}^{\infty}\mathrm{Im}\left[\int_{-\infty}^{\infty}\frac{d\omega}{2\pi}f(\omega)\mathcal{A}_{l+1,l}(k,\omega)\right]. \tag{29}$$

Note that in previous works[6–8] we have evaluated the dc current from a representation in terms of the retarded Green's function $G^R_{l,l'}(t,\omega)$. Instead, the expressions (22) and (29) are based in a representation in terms of the Fourier components of the Green's functions, which is adequate provided that a direct method for the evaluation of those components is employed in the solution of the Dyson equation. This is a convenient route to follow in combination with the renormalization procedure introduced in Sec. IV. Let us also mention that the currents flowing through the leads can also be expressed in terms of the functions $\hat{\mathcal{G}}(k,\omega)$, as shown in Ref. 30. Of course, due to the conservation of the charge, in a two-terminal setup, the result obtained for the dc current flowing through the leads connecting the central system to left and right reservoirs do coincide with the current J_l^{dc} evaluated from (29).

IV. RENORMALIZATION PROCEDURE TO EVALUATE RETARDED GREEN'S FUNCTION

In this section, we present an efficient method to solve the Dyson equation for the retarded Green's function (11) by recourse to a systematic elimination of frequency modes with the subsequent renormalization of the effective interactions and Green's functions. Although the method is general, due to pedagogical reasons, we explain the procedure for the cases of time-periodic systems oscillating with one and two harmonic components.

A. Single harmonic case

This case corresponds to $\hat{V}_k^+(\omega)=\hat{V}_k^-(\omega)=0$, $k\geq 2$. Our aim is the calculation of the Fourier components $\hat{\mathcal{G}}(k,\omega)$ at a given frequency ω.

The first step is to define a cutoff K, which determines the number of coupled frequencies $\omega-K\Omega_0,\ldots,\omega,\ldots,\omega+K\Omega_0$ and, thus, the total number of coupled equations (11).

By definition of the cutoff, the equations of the set (11) that are centered at the highest frequency $\omega+K\Omega_0$, couple only with the ones centered at $\omega+(K-1)\Omega_0$:

$$\hat{G}^R(t,\omega+K\Omega_0)[\hat{G}^0(\omega+K\Omega_0)]^{-1} = \hat{1} + e^{i\Omega_0 t}\hat{G}^R(t,\omega+(K-1)\Omega_0)\hat{V}_1^+(\omega+K\Omega_0). \quad (30)$$

Therefore, the Green's functions $\hat{G}^R(t,\omega+K\Omega_0)$ may be expressed in terms of $\hat{G}^R(t,\omega+(K-1)\Omega_0)$ and can be eliminated by substituting the ensuing expression into the equations centered at $\omega+(K-1)\Omega_0$,

$$\hat{G}^R(t,\omega+(K-1)\Omega_0)(\{\hat{G}^0[\omega+(K-1)\Omega_0]\}^{-1} - \hat{V}_1^+(\omega+K\Omega_0)\hat{G}^0(\omega+K\Omega_0)\hat{V}_1^-[\omega+(K-1)\Omega_0])$$

$$= \hat{1} + e^{i\Omega_0 t}\hat{G}^R[t,\omega+(K-2)\Omega_0]\hat{V}_1^+[\omega+(K-1)\Omega_0] + e^{-i\Omega_0 t}\hat{G}^0(\omega+K\Omega_0)\hat{V}_1^-[\omega+(K-1)\Omega_0]. \quad (31)$$

This process can be repeated, systematically eliminating high-frequency modes.

Analogously, it is possible to start with the equations centered at the lowest-frequency cutoff $\omega-K\Omega_0$

$$\hat{G}^R(t,\omega-K\Omega_0)[\hat{G}^0(\omega-K\Omega_0)]^{-1} = \hat{1} + e^{-i\Omega_0 t}\hat{G}^R(t,\omega-(K-1)\Omega_0)\hat{V}_1^-(\omega-K\Omega_0), \quad (32)$$

and implement a similar back-substitution scheme to eliminate the low-frequency modes.

At the mth step, the expressions for the eliminated high- (low-) frequency modes read

$$\hat{G}^R(t,\omega\pm m\Omega_0)[\hat{g}^{(\pm m)}(\omega\pm m\Omega_0)]^{-1} = \hat{1} + e^{\pm i\Omega_0 t}\hat{G}^R[t,\omega\pm(m-1)\Omega_0]\hat{V}_1^{\pm}(\omega\pm m\Omega_0) + e^{\mp i\Omega_0 t}\hat{\gamma}^{(\pm m)}(t,\omega). \quad (33)$$

Note that Eqs. (30)–(33) exhibit an identical structure. At each step of the mode elimination, the inverse of the "bare" Green's function $\hat{G}^0(\omega\pm m\Omega_0)$ renormalizes as follows:

$$[\hat{g}^{(\pm m)}(\omega\pm m\Omega_0)]^{-1} = [\hat{G}^0(\omega\pm m\Omega_0)]^{-1} - \hat{V}_1^{\pm}[\omega\pm(m+1)\Omega_0] \times \hat{g}^{(\pm m\pm 1)}[\omega\pm(m+1)\Omega_0]\hat{V}_1^{\mp}(\omega\pm m\Omega_0), \quad (34)$$

with $\hat{g}^{(\pm K)}(\omega\pm K\Omega_0)\equiv\hat{G}^0(\omega\pm K\Omega_0)$. The right-hand side also renormalizes as

$$\hat{\gamma}^{(\pm m)}(t,\omega) = [\hat{1} + e^{\mp i\Omega_0 t}\hat{\gamma}^{(\pm m\pm 1)}(t,\omega)]\hat{g}^{(\pm m\pm 1)}[\omega\pm(m+1)\Omega_0]\hat{V}_1^{\mp}(\omega\pm m\Omega_0), \quad (35)$$

with $\gamma^{(\pm K)}(t,\omega)\equiv 0$, which, in practice, generates an expansion in harmonics with Fourier components that renormalize at each step. The method is pictorially represented in the scheme of Fig. 1.

Finally, repeating K steps the elimination of higher- and lower-frequency modes, leads us to the following goal:

$$\hat{G}^R(t,\omega) = \sum_{k=-K}^{K}\hat{\mathcal{G}}(k,\omega)e^{-ik\Omega_0 t}, \quad (36)$$

being

$$\hat{\mathcal{G}}(0,\omega) = \{[\hat{G}^0(\omega)]^{-1} - \hat{V}_1^+(\omega+\Omega_0)\hat{g}^{(+1)}(\omega+\Omega_0)\hat{V}_1^-(\omega) - \hat{V}_1^-(\omega-\Omega_0)\hat{g}^{(-1)}(\omega-\Omega_0)\hat{V}_1^+(\omega)\}^{-1},$$

$$\hat{\mathcal{G}}(k,\omega) = \hat{g}^{(+k)}(\omega+k\Omega_0)\hat{V}_1^-[\omega+(k-1)\Omega_0]\hat{\mathcal{G}}(k-1,\omega), \quad k>0,$$

$$\hat{\mathcal{G}}(k,\omega) = \hat{g}^{(-|k|)}(\omega+k\Omega_0)\hat{V}_1^+[\omega+(k+1)\Omega_0]\hat{\mathcal{G}}(k+1,\omega), \quad k<0. \quad (37)$$

Note that the whole procedure is based in operations with small matrices of size $N\times N$.

B. Biharmonic case

This case corresponds to $\hat{V}_k^+(\omega)=\hat{V}_k^-(\omega)=0$, $k\geq 3$. The mechanics of the method is identical to the one described in Sec. IV A and can be also pictorially represented by a similar scheme (see Fig. 2). The difference with respect to the single-harmonic case is the additional renormalization of the interactions $V_1^{\pm}(\omega)$ at each step of the mode elimination. Although this case is algebraically harder, it is possible to obtain explicit expressions for its solution. In particular, the eliminated high- (low-) frequency mode at the m*th* step reads

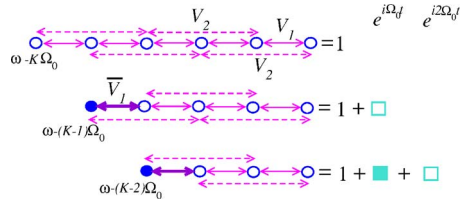

FIG. 2. (Color online) Scheme of the first steps of the low-frequency mode elimination for a biharmonic Hamiltonian. Details are similar to Fig. 1. The two harmonic components are indicated with V_1, V_2 and dashed and solid lines, respectively. In this case, the mode elimination renormalizes the interaction V_1, which is indicated with a thicker line.

$$\hat{G}^R(t,\omega\pm m\Omega_0)[\hat{g}^{(\pm m)}(\omega\pm m\Omega_0)]^{-1}=\hat{1}+e^{\pm i\Omega_0 t}\hat{G}^R[t,\omega\pm(m-1)\Omega_0]\hat{V}_1^{\pm}(\pm m,\omega\pm m\Omega_0)+e^{\pm i2\Omega_0 t}\hat{G}^R \times(t,\omega\pm(m-2)\Omega_0)\hat{V}_2^{\pm}(\omega\pm m\Omega_0)+e^{\mp i\Omega_0 t}\hat{\gamma}_1^{(\pm m)}(t,\omega)+e^{\mp i2\Omega_0 t}\hat{\gamma}_2^{(\pm m)}(t,\omega), \tag{38}$$

being

$$[\hat{g}^{(\pm m)}(\omega\pm m\Omega_0)]^{-1}=\hat{G}^0(\omega\pm m\Omega_0)^{-1}-\hat{V}_1^{\pm}[\pm(m+1),\omega\pm(m+1)\Omega_0]\hat{g}^{(\pm m\pm 1)}[\omega\pm(m+1)\Omega_0]\hat{V}_1^{\mp}[\pm(m+1),\omega\pm m\Omega_0] \times-\hat{V}_2^{\pm}[\omega\pm(m+2)\Omega_0]\hat{g}^{(\pm m\pm 2)}[\omega\pm(m+2)\Omega_0]\hat{V}_2^{\mp}(\omega\pm m\Omega_0), \tag{39}$$

with $\hat{g}^{(\pm K)}(\omega\pm K\Omega_0)\equiv\hat{G}^0(\omega\pm K\Omega_0)$, while

$$\hat{\gamma}_1^{(\pm m)}(t,\omega)=[\hat{1}+e^{\mp i\Omega_0 t}\hat{\gamma}_1^{(\pm m\pm 1)}(t,\omega)+e^{\mp i2\Omega_0 t}\hat{\gamma}_2^{(\pm m\pm 1)}(t,\omega)]\hat{g}^{(\pm m\pm 1)}[\omega\pm(m+1)\Omega_0]\hat{V}_1^{\mp}[\pm(m+1),\omega\pm m\Omega_0],$$

$$\hat{\gamma}_2^{(\pm m)}(t,\omega)=[\hat{1}+e^{\mp i\Omega_0 t}\hat{\gamma}_1^{(\pm m\pm 2)}(t,\omega)+e^{\mp i2\Omega_0 t}\hat{\gamma}_2^{(\pm m\pm 2)}(t,\omega)]\hat{g}^{(\pm m\pm 2)}[\omega\pm(m+2)\Omega_0]\hat{V}_2^{\mp}(\omega\pm m\Omega_0), \tag{40}$$

being $\gamma_1^{(\pm K)}(t,\omega)=\gamma_2^{(\pm K)}(t,\omega)=\gamma_2^{(\pm K\mp 1)}(t,\omega)\equiv 0$. The interaction $V_1^{\pm}$ renormalizes as

$$\hat{\mathcal{V}}_1^{+}(m,\omega+m\Omega_0)=V_1^{+}(\omega+m\Omega_0)+V_2^{+}[\omega+(m+1)\Omega_0]\hat{g}^{+(m+1)}[\omega+(m+1)\Omega_0]\hat{\mathcal{V}}_1^{-}(m+1,\omega+m\Omega_0),$$

$$\hat{\mathcal{V}}_1^{-}(m+1,\omega+m\Omega_0)=V_1^{-}(\omega+m\Omega_0)+\hat{\mathcal{V}}_1^{+}[m+2,\omega+(m+2)\Omega_0]\hat{g}^{+(m+2)}[\omega+(m+2)\Omega_0]V_2^{-}(\omega+m\Omega_0), \tag{41}$$

along the high-frequency elimination steps and

$$\hat{\mathcal{V}}_1^{-}(-m,\omega-m\Omega_0)=V_1^{-}(\omega-m\Omega_0)+V_2^{-}[\omega-(m+1)\Omega_0]\hat{g}^{-(m+1)}[\omega-(m+1)\Omega_0]\hat{\mathcal{V}}_1^{+}[-(m+1),\omega-m\Omega_0],$$

$$\hat{\mathcal{V}}_1^{+}[-(m+1),\omega-m\Omega_0]=V_1^{+}(\omega-m\Omega_0)+\hat{\mathcal{V}}_1^{-}[-(m+2),\omega-(m+2)\Omega_0]\hat{g}^{-(m+2)}[\omega-(m+2)\Omega_0]V_2^{+}(\omega-m\Omega_0), \tag{42}$$

for the low-frequency elimination steps.

The elimination of high- and low-frequency modes explained above has to be repeated $K-1$ steps. The equations centered at $\omega\pm\Omega_0$ and ω must be considered separately. The final solution for the Fourier component $k=0$ reads

$$\hat{\mathcal{G}}(0,\omega)=\{[\hat{G}^0(\omega)]^{-1}-\hat{V}_2^{+}(\omega+2\Omega_0)\hat{g}^{(+2)}(\omega+2\Omega_0)\hat{V}_2^{-}(\omega)-\hat{V}_2^{-}(\omega-2\Omega_0)\hat{g}^{(-2)}(\omega-2\Omega_0)\hat{V}_2^{+}(\omega)-\hat{\hat{\mathcal{V}}}_1^{-}(\omega-\Omega_0)\hat{\bar{g}}^{(-1)}(\omega-\Omega_0)\hat{\mathcal{V}}_1^{+}(-1,\omega)-\hat{\hat{\mathcal{V}}}_1^{+}(\omega+\Omega_0)\hat{\bar{g}}^{(+1)}(\omega+\Omega_0)\hat{\mathcal{V}}_1^{-}(1,\omega)\}^{-1}, \tag{43}$$

where

$$\hat{\bar{g}}^{(+1)}(\omega+\Omega_0)=\{[\hat{g}^{(+1)}(\omega+\Omega_0)]^{-1}-\hat{V}_2^{-}(\omega-\Omega_0)\hat{g}^{(-1)}(\omega-\Omega_0)\hat{V}_2^{+}(\omega+\Omega_0)\}^{-1},$$

$$\hat{\bar{g}}^{(-1)}(\omega-\Omega_0)=\{[\hat{g}^{(-1)}(\omega-\Omega_0)]^{-1}-\hat{V}_2^{+}(\omega+\Omega_0)\hat{g}^{(+1)}(\omega+\Omega_0)\hat{V}_2^{-}(\omega-\Omega_0)\}^{-1}, \tag{44}$$

and

$$\hat{\hat{\mathcal{V}}}_1^{-}(\omega-\Omega_0)=\hat{\mathcal{V}}_1^{-}(-1,\omega-\Omega_0)+\hat{\mathcal{V}}_1^{+}(1,\omega+\Omega_0)\hat{g}^{(+1)}(\omega+\Omega_0)\hat{V}_2^{-}(\omega-\Omega_0),$$

$$\hat{\hat{\mathcal{V}}}_1^{+}(\omega+\Omega_0)=\hat{\mathcal{V}}_1^{+}(1,\omega+\Omega_0)+\hat{\mathcal{V}}_1^{-}(-1,\omega-\Omega_0)\hat{g}^{(-1)}(\omega-\Omega_0)\hat{V}_2^{+}(\omega+\Omega_0). \tag{45}$$

The remaining Fourier components are

$$\hat{\mathcal{G}}(-1,\omega)=[\hat{\bar{g}}^{(-1)}(\omega-\Omega_0)\hat{\mathcal{V}}_1^{+}(-1,\omega)+\hat{g}^{(-1)}(\omega-\Omega_0)\hat{V}_2^{+}(\omega+\Omega_0)\hat{\bar{g}}^{(+1)}(\omega+\Omega_0)\hat{\mathcal{V}}_1^{-}(1,\omega)]\hat{\mathcal{G}}(0,\omega),$$

$$\hat{\mathcal{G}}(1,\omega) = [\hat{\bar{g}}^{(+1)}(\omega+\Omega_0)\hat{V}_1^-(1,\omega) + \hat{g}^{(+1)}(\omega+\Omega_0)\hat{V}_2^-(\omega-\Omega_0)\hat{\bar{g}}^{(-1)}(\omega-\Omega_0)\hat{V}_1^+(-1,\omega)]\hat{\mathcal{G}}(0,\omega), \tag{46}$$

and

$$\hat{\mathcal{G}}(k,\omega) = \hat{g}^{(-|k|)}(\omega+k\Omega_0)[\hat{V}_2^+(\omega+(k+2)\Omega_0)\hat{\mathcal{G}}(k+2,\omega) + \hat{\mathcal{V}}_1^+(k,\omega+(k+1)\Omega_0)\hat{\mathcal{G}}(k+1,\omega)], \quad k \leq -2,$$

$$\hat{\mathcal{G}}(k,\omega) = \hat{g}^{(+k)}(\omega+k\Omega_0)[\hat{V}_2^-(\omega+(k-2)\Omega_0)\hat{\mathcal{G}}(k-2,\omega) + \hat{\mathcal{V}}_1^-(k,\omega+(k-1)\Omega_0)\hat{\mathcal{G}}(k-1,\omega)], \quad k \geq 2. \tag{47}$$

The mechanics of the method can be generalized to the case of n harmonic components, with $n>2$. Each step of the mode elimination would involve the renormalization of the inverse of the "bare" retarded Green's function, as well as the interactions $\hat{V}^{\pm}(k,\omega); k=1,\ldots,n-1$ and the coefficients $\hat{\gamma}_k(t,\omega); k=1,\ldots,n$. The procedure has to be followed along $K-(n+1)$ steps, and the equations centered at $\omega-(n-1)\Omega_0,\ldots,\omega,\ldots,\omega+(n-1)\Omega_0$, have to be treated separately. Relations such as (47) would be obtained for $|k| \geq n$ and would relate $\hat{\mathcal{G}}(k,\omega)$ with $\hat{\mathcal{G}}(k\pm 1,\omega),\ldots,\hat{\mathcal{G}}(k\pm n,\omega)$.

V. EXAMPLE

In what follows, we illustrate the method introduced in Sec. IV in the simple problem of a double barrier structure oscillating with two harmonic components. The central system is described by a Hamiltonian of the form (2) with

$$\varepsilon_{l,l'} = -w\delta_{l',l+1} + E_{b_1}\delta_{l,l'}\delta_{l,l_1} + E_{b_2}\delta_{l,l'}\delta_{l,l_2}, \tag{48}$$

where l_1, l_2 denote the positions of the barriers. The time-dependent components are

$$V_{l,l'}(t) = \delta_{l,l'}\delta_{l,l_1}[V_1\cos(\Omega_0 t+\delta) + V_2\cos(2\Omega_0 t+\delta)] + \delta_{l,l'}\delta_{l,l_2}[V_1\cos(\Omega_0 t) + V_2\cos(2\Omega_0 t)]. \tag{49}$$

For simplicity, we consider a configuration where the central system is placed in between two static left (L) and right (R) reservoirs with the same chemical potential μ, and $V_\alpha = 0$, being $\alpha = L, R$. We consider infinite tight-binding chains with hopping element $W/2$ as models of reservoirs, which corresponds to $\Gamma_\alpha(\omega) = |w_\alpha|^2 4\Theta(|\omega|-W)\sqrt{\omega^2-W^2}$. We work with $\hbar=1$, and energy and frequency values are expressed in units of the hopping parameter w. We have selected the following parameters of the model: $N=20$, $E_b=1$, $w_\alpha^2=0.5$, and $W=4$. The results shown in Figs. 3–5 correspond to a phase-lag $\delta=\pi/2$ between the two oscillating fields.

We have implemented the renormalization procedure presented in Sec. IV in a numerical code. The numerical values $K=10$ to $K=20$ for the parameter defining the cutoff, were found to be enough, depending on the pumping amplitudes and frequencies. In general, the optimum K corresponds to the minimum value of this parameter, such that the numerical estimate of the Green's function does not differ (within the machine precision) from the one calculated with a larger K. The most demanding cases correspond to large pumping amplitudes and pumping frequencies Ω_0 close to resonance, i.e., approximately equal to the energy difference between two energy levels of the central structure. In our model, this condition is achieved, for example, when $\Omega_0 \sim 0.3$.

The typical behavior of the first k components of the spectral density of occupation $\mathcal{A}_{l_1,l_1}(k,\omega)$ at one of the sites where the driving potential is applied is illustrated in Figs. 3 and 4, for the case of low pumping frequency and amplitude, and a pumping frequency close to resonance and higher amplitude, respectively.

In the case of low driving amplitude and frequency shown in Fig. 3, the $k=0$ component shown in the upper panel is clearly the dominating contribution to the total spectral density of occupation $\bar{\rho}_{l_1,l_1}(0,\omega)$. In this case, $\mathcal{A}_{l_1,l_1}(0,\omega)$ does not depart strongly from the behavior of the local density of states of the equilibrium system, which is shown in dashed

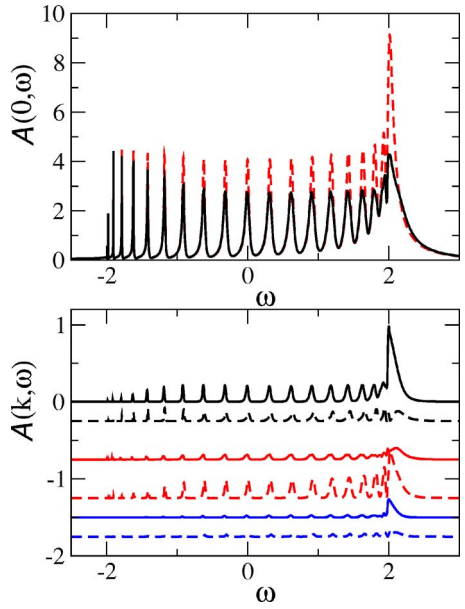

FIG. 3. (Color online) The spectral density $\mathcal{A}_{l_1,l_1}(k,\omega)$. Upper panel corresponds to $k=0$ (solid line). The local density of states at the same position of the equilibrium system is also plotted for comparison in the dashed line. Lower panel corresponds to $k=\pm 1,\pm 2,\pm 3$ (top to bottom), where $k>0$ ($k<0$) are depicted in solid (dashed) lines, respectively. The parameters for the pumping potentials are $V_1=V_2=0.2$ with $\Omega_0=0.01$ and $\delta=0.5\pi$. The coupling to the reservoir is $|w_L|^2=|w_R|^2=0.5$, and the wideband of the reservoir is $W=4$. To facilitate visualization, the plots of the lower panel contain vertical shifts equal to $-0.25, -0.75, -1.25, -1.5$, and -1.75 (top to bottom plots). Other parameters are the same as in Fig. 3.

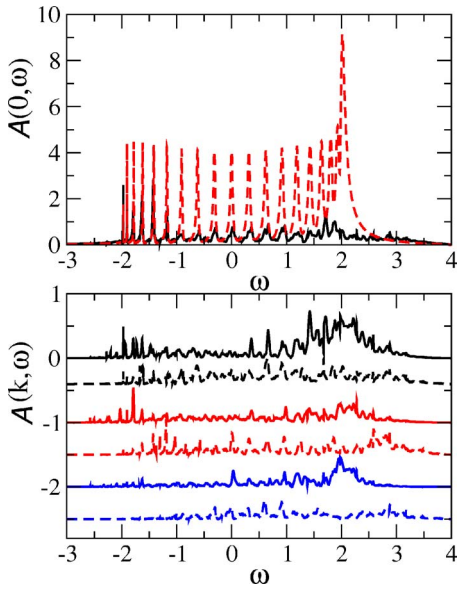

FIG. 4. (Color online) The same as 3 for $V_1=V_2=1$ with $\Omega_0=0.3$. To facilitate visualization, the plots of the lower panel contain vertical shifts equal to $-0.4,-1,-1.5,-2,-2.5$ (top to bottom plots). Other parameters are the same as in Fig. 3.

lines for comparison. The other sizable components, shown in the lower panel, correspond to $k=\pm 1$ and $k\pm 2$, which coincide with the nonvanishing harmonic components of the driving field, while components with higher $|k|$ (see, e.g., $k=\pm 3$) have an almost negligible weight at all energies ω. It is also interesting to note that the functions $\mathcal{A}_{l_1,l_1}(k,\omega)$, as functions of ω, exhibit peaks at, roughly, the same positions at which the central structure has resonant levels, as becomes apparent from the comparison to the density of states for the system at equilibrium. Recalling that the sum rule (25) is also satisfied by the spectral density of states of the equilibrium system, the behavior of the spectral functions shown in Fig. 3 suggests that the effect of the driving can be interpreted as a spread of the equilibrium density of states in a dominant component $[\mathcal{A}_{l_1,l_1}(0,\omega)]$ plus "side" components corresponding to $k=\pm 1,\pm 2$. This means that the spectral density of occupation $\bar{\rho}_{l_1,l_1}(0,\omega)$ (not shown), being a superposition of all the functions $\mathcal{A}_{l_1,l_1}(k,\omega)$ differs, in this case, only mildly from the equilibrium density of states. Also, since the nonequilibrium density of states $\rho_{l_1,l_1}(0,\omega)$ (not shown) is the superposition of the functions $\mathcal{A}_{l_1,l_1}(k,\omega-k\Omega_0)$, and being $k\Omega_0$ small for the low-k components, in the low driving and frequency case of Fig. 3 $\rho_{l_1,l_1}(0,\omega)\sim\bar{\rho}_{l_1,l_1}(0,\omega)$, and the two densities are, in turn, very similar to the equilibrium density of states. Thus, in the weak and slow driving regime, the nonequilibrium behavior manifests itself at the level of the local electronic population only through time-dependent oscillations, while the dc features do not significantly differ from those of the equilibrium system.

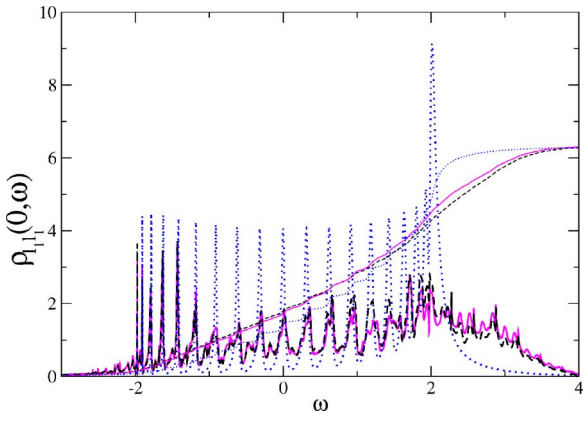

FIG. 5. (Color online) The local density of states $\rho_{l_1,l_1}(0,\omega)$ at one of the points of application of the pumping potential in solid magenta (gray) and the local density of occupation $\bar{\rho}_{l_1,l_1}(0,\omega)$ in dashed black line. For comparison, the equilibrium density of states is also shown in dotted lines. The corresponding integral of these functions is also plotted in thinner lines, using the same colors and line types. The parameters corresponding to the oscillating fields are $V_1=V_2=1$ with $\Omega_0=0.3$ and $\delta=\pi/2$. Other parameters are the same as in Fig. 3.

Figure 4 exhibits the behavior of the spectral functions $\mathcal{A}_{l_1,l_1}(k,\omega)$ for a higher pumping amplitude and a frequency Ω_0 close to resonance. In the upper panel, the density of states at the site l_1 corresponding to the equilibrium system is also indicated for reference. In this case, there is a strong decomposition of the equilibrium spectral weight not only along the different k components but also the peaks of the equilibrium density of states split developing additional structure along the ω axis. The behavior of the corresponding densities of states and of occupation $\rho_{l_1,l_1}(0,\omega)$ and $\bar{\rho}_{l_1,l_1}(0,\omega)$, respectively, is shown in Fig. 5. The equilibrium density of states is also shown in this case for comparison. In contrast to the weak driving and low-frequency case shown in Fig. 3, the two spectral densities are clearly different in this case and both functions strongly differ from the equilibrium one. An important feature is that while in equilibrium the available energy states to be occupied by electrons are confined around a sequence of sharp resonances, several new peaks are generated in the driven system. In particular, several new states merge above the top of the band of the equilibrium system. As a consequence, the effect of the driving is not only to induce a current across the structure but for sizable amplitudes of the oscillating field and resonant frequencies, it also strongly affects other experimental features related to the local energy-resolved electronic population.

To finalize, let us present results for the behavior of the induced dc current J^{dc} defined in (29) as a function of the phase lag δ (note that due to charge conservation, the dc current is in this case independent of l). Let us recall that for a single harmonic component ($V_2=0$) and weak driving amplitude V_1, as well as for low pumping frequencies, the dc current depends on the phase-lag as $J^{dc}\propto\sin(\delta)$.[7,8,10] For small V_1,V_2, the same perturbative treatment employed in Refs. 7 and 8 can be employed to calculate the dc current and the same functional dependence on δ is found. However, for larger driving amplitudes, J^{dc} as a function of δ can strongly depart from that behavior, as shown in Fig. 6, where the upper panel corresponds to a low frequency, whereas the lower one corresponds to a frequency close to resonance. The most salient feature is that $J^{dc}\neq 0$ for $\delta=\pi$, in contrast to the behavior observed in the case of single harmonic

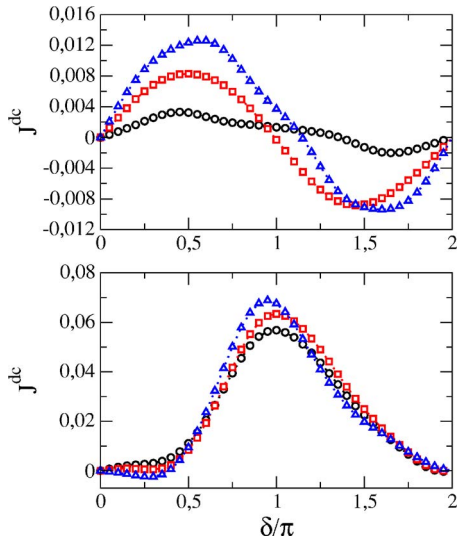

FIG. 6. (Color online) The dc current as a function of the phase-lag δ for $V_1=V_2=1$ and $\Omega_0=0.1$ (upper panel) and $\Omega_0=0.3$ (lower panel). The different plots in circles, squares, and triangles correspond to different values of the chemical potential $\mu=-1.5,-1.42$, and -1.22, respectively. Other parameters are the same as in Fig. 3.

driving.[7,8] This issue can be understood on the basis of a symmetry analysis originally proposed for classical ratchets[31] and employed to analyze the transport behavior of quantum pumps in Ref. 8. Following Ref. 31, in order to conclude about the vanishing of J^{dc}, we have to look for symmetries of the relevant equation of motion that cause the inversion of the sign of the time-dependent current. The relevant symmetries to analyze are time inversion $t\rightarrow -t$ and spatial inversion. The first symmetry is broken due to the coupling to reservoirs, as discussed in Ref. 8. For the case of a symmetric structure and identical pumping amplitudes applied at two symmetric points analyzed in this work, H^{sys} is invariant under spacial inversion with respect to an axis through the center of the structure only for the particular values of the phase-lag $\delta=mod(2\pi)$. Since the latter symmetry operation changes the sign of the time-dependent current, this explains that $J^{dc}=0$ at these points. In the case of potentials oscillating with a single harmonic component, there is an additional symmetry of H^{sys} at $\delta=\pi$ that consists of the simultaneous spacial inversion and a shift in time: $t\rightarrow t-\delta/\Omega_0$. Such symmetry also changes the sign of the time-dependent current, thus explaining the vanishing J^{dc} at $\delta=\pi$ in the single-harmonic case. This symmetry is, however, broken when the driving field oscillates with more than one harmonic component, which explains the finite dc current at $\delta=\pi$ observed in Fig. 6. Remarkably, at resonant frequencies (see lower panel of Fig. 6) the effect of the second harmonic is to provide a mechanism to change the sign of the dc current within the range $\pi<\delta<2\pi$. Furthermore, the point $\delta=\pi$ at which the dc current vanishes in the single-harmonic case turns to become a maximum.

VI. SUMMARY AND DISCUSSION

We have introduced a practical method to evaluate the retarded Green's function in problems described by Hamiltonians of noninteracting fermions with harmonically time-dependent terms. The method is based in the subsequent elimination of high- and low-frequency modes. The procedure generates effective renormalized interactions and recursive relations between the Green's functions, allowing for explicit expressions for the different Fourier components. We have also presented a discussion on the possibility and usefulness of defining spectral functions that play the role of generalized densities of states and of occupation in situations where the reservoirs to which a locally driven system is connected are stationary and have the same temperature and chemical potentials. We have illustrated the algorithm in a model of a quantum pump driven by biharmonic local potentials oscillating with a phase lag. These results allowed us to further analyze the fundamental role played by symmetries in enabling or disabling mechanisms for the generation of directed currents.

From the computational point of view, the presented method defines a fast algorithm to directly evaluate the Fourier components of the Green's functions on the basis of operations with small matrices. Typical computational times for the simple model considered in Sec. V are approximately 15 min in a workstation for any of the plots shown in Fig. 3–5, which cover a wide range of pumping frequencies and amplitudes.

We would like to stress that several interesting time-dependent problems (such as the quantum pumps with multiharmonic driving considered in Sec. V, problems with oscillating reservoirs, or rings driven with time-dependent magnetic fluxes that depart from the simple linear time-dependence) imply dealing with several coupling terms $V^{\pm}_{l,l'}(k,\omega)$ in Eq. (11). The numerical study of time-dependent problems in open systems with disorder would be based in the solution of the Dyson equation for several realizations of disorder, which is computationally very demanding, even in the simplest case of a single harmonic component. Such problems would not be, in practice, computationally available unless efficient algorithms are employed to solve the Dyson equation.

The mechanics of the method resembles the one employed to solve recursively the Dyson equation of the retarded Green's function in real space in the context of stationary or equilibrium problems.[18–23] Since the latter methodology proved to be practical and useful in the implementation of *ab initio* methods, we also expect that our method will also be useful in the development of *ab initio* treatments to investigate details of systems in the presence of time-oscillating external fields, such as surfaces attacked by lasers and molecular bridges driven by ac fields.

ACKNOWLEDGMENTS

Support from PICT Grant No. 03-11609 and CONICET from Argentina, Grant No. BFM2003-08532-C02-01 from MCEyC of Spain, grant "Grupo de Excelencia DGA," and from the MCEyC of Spain through the "Ramon y Cajal" program are acknowledged.

[1] L. J. Geerligs, V. F. Anderegg, P. A. M. Holweg, J. E. Mooij, H. Pothier, D. Esteve, C. Urbina, and M. H. Devoret, Phys. Rev. Lett. **64**, 2691 (1990); L. DiCarlo, C. M. Marcus, and J. S. Harris, *ibid.* **91**, 246804 (2003); M. Switkes, C. M. Marcus, K. Campman, and A. C. Gossard, Science **293**, 1905 (1999); S. K. Watson, R. M. Potok, C. M. Marcus, and V. Umansky, Phys. Rev. Lett. **91**, 258301 (2003).

[2] V. Chandrasekhar, R. A. Webb, M. J. Brady, M. B. Ketchen, W. J. Gallagher, and A. Kleinsasser, Phys. Rev. Lett. **67**, 3578 (1991); D. Mailly, C. Chapelier, and A. Benoit, *ibid.* **70**, 2020 (1992); R. Deblock, R. Bel, B. Reulet, H. Bouchiat, and D. Mailly, *ibid.* **89**, 206803 (2002).

[3] P. J. Leek, M. R. Buitelaar, V. I. Talyanskii, C. G. Smith, D. Anderson, and G. A. C. Jones, J. Wei, and D. H. Cobden, Phys. Rev. Lett. **95**, 256802 (2005).

[4] C. T. Liu, J. M. Liu, P. A. Garbinski, S. Luryi, D. L. Sivco, and A. Y. Cho, Phys. Rev. Lett. **67**, 2231 (1991); A. C. Morteani, P. Sreearunothai, L. M. Herz, R. H. Friend, and C. Silva, *ibid.* **92**, 247402 (2004); V. D. Mihailetchi, L. J. A. Koster, J. C. Hummelen, and P. W. M. Blom, *ibid.* **93**, 216601 (2004).

[5] K. B. Nordstrom, K. Johnsen, S. J. Allen, A.-P. Jauho, B. Birnir, J. Kono, T. Noda, H. Akiyama, and H. Sakaki, Phys. Rev. Lett. **81**, 457 (1998).

[6] L. Arrachea, Phys. Rev. B **66**, 045315 (2002); L. Arrachea, Eur. Phys. J. B **36**, 253 (2003); L. Arrachea, Phys. Rev. B **70**, 155407 (2004); L. Arrachea and L. Cugliandolo, Europhys. Lett. **70**, 642 (2005).

[7] L. Arrachea, Phys. Rev. B **72**, 125349 (2005).

[8] L. Arrachea, Phys. Rev. B **72**, 121306(R) (2005); **72**, 249904(E) (2005).

[9] V. I. Yudson, E. Kanzieper, and V. E. Kravtsov, Phys. Rev. B **64**, 045310 (2001).

[10] M. Moskalets and M. Büttiker, Phys. Rev. B **66**, 205320 (2002).

[11] G. Platero and R. Aguado, Phys. Rep. **395**, 1 (2004).

[12] S. Kohler, J. Lehmann, and P. Hänggi, Phys. Rep. **406**, 379 (2005).

[13] L. E. F. Foa Torres, Phys. Rev. B **72**, 245339 (2005).

[14] S. Kim, K. K. Das, and A. Mizel, Phys. Rev. B **73**, 075308 (2006).

[15] C. Caroli, R. Combescot, P. Nozieres, and D. Saint-James, J. Phys. C **4**, 916 (1971).

[16] A.-P. Jauho, N. S. Wingreen, and Y. Meir, Phys. Rev. B **50**, 5528 (1994).

[17] H. M. Pastawski, Phys. Rev. B **46**, 4053 (1992).

[18] E-N Foo, M. F. Thorpe, and D. Weaire, Surf. Sci. **57**, 323 (1976).

[19] C. E. T. Gonzalves da Silva and B. Koiller, Solid State Commun. **40**, 215 (1981).

[20] D. J. Thouless and S. Kirkpatrick, J. Phys. C **14**, 235 (1981).

[21] D. H. Lee and J. D. Joannopoulos, Phys. Rev. B **23**, 4988 (1981).

[22] F. Guinea, C. Tejedor, F. Flores, and E. Louis, Phys. Rev. B **28**, 4397 (1983).

[23] F. Sols, M. Macucci, U. Ravaioli, and K. Hess, J. Appl. Phys. **66**, 3892 (1989).

[24] A. A. Abrikosov, L. P. Gorkov, and I. E. Dzyaloshinski, *Methods of Quantum Field Theory in Statistical Physics* (Dover, New York, 1975); G. D. Mahan, *Many-Particle Physics*, Plenum Press, New York (1990).

[25] B. Wang, J. Wang, and H. Guo, Phys. Rev. B **68**, 155326 (2003).

[26] A. P. Jauho and K. Johnsen, Phys. Rev. Lett. **76**, 4576 (1996).

[27] H. Pothier, S. Guéron, Norman O. Birge, D. Esteve, and M. H. Devoret, Phys. Rev. Lett. **79**, 3490 (1997).

[28] A. Komnik and A. O. Gogolin, Phys. Rev. B **66**, 035407 (2002).

[29] D. G. Barci, L. Moriconi, M. Moriconi, C. M. Naón, and M. J. Salvay, Phys. Rev. B **72**, 235112 (2005).

[30] L. Arrachea and M. Moskalets, cond-mat/0607278 (unpublished).

[31] S. Flach, O. Yevtushenko, and Y. Zolotaryuk, Phys. Rev. Lett. **84**, 2358 (2000).